TITLE: Can skeletal surface area predict in vivo foot surface area?

AUTHORS: Strickson, E C; Hutchinson, J R; Wilkinson, D M; Falkingham, P L

JOURNAL: genesis: Journal of Anatomy

PUBLISHER: Wiley

PUBLICATION DATE: 12 November 2019

DOI: https://doi.org/10.1111/joa.13090

Can Skeletal Surface Area Predict *in vivo* Foot Surface Area?

E. Catherine Strickson[1], John R. Hutchinson[2], David M. Wilkinson[3] and Peter L. Falkingham[1]

[1]School of Natural Sciences and Psychology, Faculty of Science, Liverpool John Moores University, Liverpool, United Kingdom.

[2]Structure and Motion Laboratory, Department of Comparative Biomedical Sciences, The Royal Veterinary College, Hatfield, United Kingdom.

[3]School of Life Sciences, College of Science, University of Lincoln, Lincoln, United Kingdom.

Corresponding Author:

E. Catherine Strickson[1]

Email address: e.strickson@2016.ljmu.ac.uk

Abstract

The surface area of feet in contact with the ground is a key morphological feature that influences animal locomotion. Underfoot pressures (and consequently stresses experienced by the foot), as well as stability of an animal during locomotion, depend on the size and shape of this area. Here we tested whether the area of a skeletal foot could predict *in vivo* soft tissue foot surface area. Computed tomography scans of 29 extant tetrapods (covering mammals, reptiles, birds and amphibians) were used to produce models of both the soft tissues and the bones of their feet. Soft tissue models were oriented to a horizontal plane, and their outlines projected onto a surface to produce two-dimensional silhouettes. Silhouettes of skeletal models were generated either from bones in CT pose or with all autopodial bones aligned to the horizontal plane. Areas of these projections were calculated using alpha shapes (mathematical tight-fitting outline). Under-foot area of soft tissue was approximately 1.67 times that of skeletal tissue area (~2 times for manus, ~1.6 times for pes, if analyzed separately). Notably high skin area relative to skeletal area was found in *Crocodylus niloticus*, and in unguligrade animals. *Coturnix, Panthera,* and *Vulpes* had lower skin relative to skeletal surface area. This relationship between skeletal foot area and soft tissue area, while variable in some of our study taxa, could provide information about the size of the organisms responsible for fossil trackways, suggest what size of tracks might be expected from potential trackmakers known only from skeletal remains, and aid in soft tissue reconstruction of skeletal remains for biomechanical modelling.

Key Words

Locomotion, ichnology, biomechanics, anatomy

Introduction

The surface area of tetrapod autopodia (feet) reflects several important biomechanical factors, including body mass (McMahon, 1975), habitat (Blackburn et al., 1999), speed (Segal et al., 2004), and bipedal or quadrupedal locomotory habits (Snyder, 1962). Foot surface area is determined by autopodial morphology and posture (Hildebrand, 1980; Full et al., 2002), and, in conjunction with the body mass and locomotory mode of an animal, determines underfoot pressure (Miller et al., 2008; Michilsens et al., 2009; Panagiotopoulou et al., 2012; Qian et al., 2013; Panagiotopoulou et al., 2016).

For very large animals, such as rhinoceroses and elephants, foot surface area needs to be large, as a method of reducing underfoot pressure and avoiding injury to the foot, as well as avoiding sinking on soft ground (Falkingham et al., 2011a). However, foot contact area does not appear to scale isometrically with mass. Larger animals often have smaller foot contact areas than would be expected, and the relationship between foot contact area and mass differs between unguligrade, digitigrade and plantigrade animals (Michelsens et al., 2009; Chi and Roth, 2010). Large animals must compensate for their size with other mechanisms, such as fatty footpads, in order to reduce stress (Panagiotopoulou et al., 2012). Presumably the extinct sauropod dinosaurs, many times larger than extant elephants (Bates et al., 2016) used similar compensatory adaptations (Platt and Hasiotis, 2006).

Foot surface area is also reflective of an animal's posture and limb use (Biewener, 1989), with bipedal animals requiring feet large enough to support their body weight with half as many limbs as their quadrupedal counterparts (Gatesy and Biewener, 1991), and, in the case of birds, in a huge range of environments and ecological niches with different demands (Alexander, 2004). An animal's balance (e.g. keeping the body's centre of mass (CoM) close to the centre of pressure of feet-- influenced by foot area) should also be considered a determining factor, as the stability of an animal during locomotion is vital to its ability to catch prey, escape predators, migrate effectively, and avoid injury when overexerting itself and when moving on unstable ground (Hodgins and Raibert, 1991; Patla, 2003; Geyer et al., 2006; Birn-Jeffery et al., 2014).

Foot surface area appears to correlate with relative speed during certain forms of locomotion. Body mass has a direct effect on maximum running speed, especially notable in large animals, as speed scales with body mass up to moderate sizes and then declines (Garland, 1983; Bejan and Marden, 2006), and the duration of foot contact with the ground also scales with body mass (Farley et al., 1993). The position and number of toes also tends to be a specialisation for terrestrial running, with a reduced number of toes present in both horses and ostriches (among other cursorial taxa; Coombs, 1978), reducing foot weight, a useful adaptation because heavier feet necessitate more energy usage to recover from a stride (Snyder, 1962; McGuigan and Wilson, 2003; Schaller, et al., 2011). Peak plantar pressure and speed are demonstrably linked in humans (Rosenbaum et al., 1994; Segal et al., 2004; Pataky et al., 2008) and ostriches (Schaller, et al., 2011); however, this link has not been fully explored in other terrestrial animals, especially quadrupeds.

Large feet have a potentially conflicting relationship with speed in that they will be more massive and thus have greater inertia, making them more difficult to swing quickly through the air (Taylor et al., 1974; Fedak et al., 1982; Kilbourne and Hoffman, 2013; Kilbourne and Carrier, 2016;). Nonetheless, it is important that foot surface area and underfoot pressures evolve to allow an organism's locomotion to be energy-efficient and its posture stable, while enabling sufficient bursts of speed if necessary. In other words, the surface area of the autopodia should be subject to selective pressures in the same manner as any other part of the locomotor system.

Foot surface area is also potentially influenced by Allen's rule (Allen, 1877; Allee and Schnidt, 1937), which supposes that warm-blooded animals in cold climates will tend to have smaller feet than their relatives in warmer clines (Blackburn et al., 1999). This may or may not be due to causal links to either reduce surface area exposed to the cold, or be a reflection of adaptations in warmer climates to increase surface area to promote heat dissipation. This rule may conflict with constraints imposed by keeping pressures low (i.e. foot areas large) to avoid sinking into soft substrates such as snow or sand. Allen's rule also potentially conflicts with the outcome of Bergmann's rule – the contentious but broadly supported tendency for ectotherms to be larger in colder climates (Clarke, 2017). Therefore, colder conditions will tend to correlate with increased body mass, implying a larger foot surface area while simultaneously selecting for smaller feet.

Some animals exhibit notable disparity in the size of fore- and hind-feet, which is apparent in their foot surface area: a condition known as heteropody. A previous study (Henderson, 2006) demonstrated that the ratio of fore- and hind-foot surface areas, in its subject animals, could match CoM position, e.g. an elephant has 40%/60% relative fore- vs. hind-foot surface area, and a CoM of 40% of the distance from the glenoid to the acetabulum. It would seem logical to assume that animals spread their body weight relatively evenly over

their feet, in order to reduce maximum pressure, excess tissue or substrate stress and strain (Cheung et al., 2005), and to prevent sinking when walking across compliant substrates (Falkingham et al., 2011a). However, this assumption runs contrary to pressure experiments showing higher mean peak pressures in elephant forelimbs (Panagiotopoulou et al., 2012). It is therefore worth exploring a possible correlation of the relative sizes of an animal's manus and pes, and CoM with both observations in mind, and worth considering possible implications of such a correlation across Tetrapoda.

Heteropody is a common occurrence in some extinct animals, such as sauropod dinosaurs, as indicated by trace fossil evidence (Lockley et al., 1994; Henderson, 2006). Preserved trackways from these dinosaurs indicate that often their fore- and hind-feet impressions differ in depth (Falkingham et al., 2010; Falkingham et al., 2012), implying differential underfoot pressures. Determining foot surface area in these animals can be complex, however, and attribution of specific trackmakers to trackways is notoriously difficult (Farlow, 1992; Clack, 1997; Falkingham, 2014), partly because matching impressions of fully fleshed feet to skeletal remains would require accurate methods of predicting skeletal to skin foot morphology, which is currently difficult and largely speculative. Indeed, matching the tracks of extant animals to the correct species is often not straightforward – as illustrated by the existence of field guides produced to help fieldworkers with this problem (e.g. Bang and Dahlstrøm, 2001).

For terrestrial and arboreal fauna, the substrate underfoot can have a noticeable effect on locomotion, and the way the foot moves in a step. Both substrate and autopodial tissue will be compressible to varying degrees, slightly altering foot contact area during stance (Gatesy, et al., 1999; Falkingham and Gatesy, 2014; Gatesy and Falkingham, 2017).

Palaeobiologists must rely on soft tissue data from extant animals to infer many facets of the morphology of extinct animals (Witmer, 1995), because preservation of soft tissues is rare and only partial details about muscle and tendon structures can be inferred from the skeletal elements they interacted with. In this way, a study of the relationship of flesh and skeletal foot surface area should help to fill gaps in our understanding of the anatomy of extinct animals' feet, as well as the interaction of foot structure and CoM, and would be particularly valuable for linking fossil trackways and supposed trackmakers. Here we aim to test whether skin and skeletal surface area are correlated across Tetrapoda, and if so, if their correlation is strong enough to make it a useful tool in the study of fossils and trackways.

Materials & Methods

In order to compare skeletal and fully fleshed foot anatomy in extant animals, computed tomography (CT) scans of cadaveric autopodia from 29 species of tetrapod (one specimen of each except for *Crocodylus moreletii* and *Osteolaemus teraspis* – see supplementary material), covering amphibians, reptiles, birds, and mammals, were analysed. The sex of individuals was unknown, and all but *Crocodylus niloticus* were adults. All specimens were museum or zoo-donated specimens whose cause of death was unrelated to this study (and generally unknown).

MeVisLab (Heckel et al., 2009) was used to segment the scans into separate 3D models (OBJ format meshes) of the soft tissue and skeletal elements. The resultant meshes were

then imported into Autodesk Maya 2018, where they were cleaned, aligned and re-posed to the horizontal plane (figure 1). The aligned meshes were then processed using MatLab (Mathworks Inc. Natick, MA, USA), where they were 'flattened' by setting the vertical component of each vertex to 0. This flattening produced 2D 'silhouettes' of the models, either as soft tissue of the foot or its skeleton, from which area was calculated using an alpha shape (see below).

Skin models were oriented and posed so that only areas of the feet that would touch the ground during locomotion would be used upon flattening the models, and any parts of the models that extended past this area were removed (figure 1B). The extent of the soles of the feet were, for the most part, obvious from visible anatomy. In addition, from *in vivo* biplanar fluoroscopy studies, X-ray images, and photographs *in situ,* we made educated estimates of accurate positions for taxa (Astley and Roberts, 2014; Bonnan, et al., 2016; Kambic et al., 2015; Panagiotopoulou, et al., 2016). For a more repeatable approach (Pose 2, see below), parts of the skin model extending past the functional foot area (the ungules for unguligrade animals, the digits for digitigrade animals, and the entire sole of the foot for plantigrade animals and semi-digitigrade animals, so that the full extent of fatty foot pads were accounted for) were removed where present.

However, since these models were taken from CT scans, without the full weight of the animal deforming the foot underneath, the true shape of the foot during stance for many of these animals may have been slightly different, due to compliant soft tissues (Alexander, et al., 1986; Gatesy and Middleton, 2003). This is especially significant for those animals with large fatty foot pads such as *Elephas* and *Ceratotherium*, and less significant for the majority of ungulates, whose hooves are stiff, and more resistant to deformation (Hinterhofer, et al., 2000; Hutchinson, et al., 2011).

Skeletal models were posed in one of two ways. Firstly (Pose 1), matching the pose of skin models (Figure 1B-D), secondly (Pose 2), with all bones aligned to the horizontal (Figure 1E-F). For the latter pose, models were cropped proximal to the digits for digitigrade animals, proximal to the unguals for unguligrade animals, proximal to the tarsals/carpals for plantigrade animals.

For large, semi-digitigrade/subunguligrade animals (*Elephas maximus, Ceratotherium simum*, and *Hippopotamus amphibius*), proximal foot elements are raised off the ground, supported by fatty foot pads, increasing foot contact area. Therefore using only the phalanges, as for other digitigrade animals, would severely underestimate contact area. To explore this ambiguity, skeletal outlines were generated from just the digits (Pose 2a), the digits plus metatarsals (Pose 2b), and with the entire foot skeleton (Pose 2c). This analysis was designed to be more objective and repeatable in determining skin from skeletal surface area, particularly, in extinct animals, where knowledge of *in vivo* foot posture may be lacking.

Results for area where left and right forefeet or hindfeet were available were averaged (mean), as were area results for animals with multiple specimens, and *Camelus,* where both feet were unassigned as forefeet or hindfeet.

It should be noted that our 29 animals studied include several ungulates, possessing large, keratinous hooves, much harder and stiffer than most other tissues categorised under 'soft tissues' in this study. While ungulate hooves have properties that distinguish them from other soft tissues, and take longer to decompose than softer tissues, they are also distinct

from skeletal tissue, and are rarely preserved, especially in fossils (Pollitt, 2004; Saitta, et al., 2017). In terms of comparisons between skeletal and fossil remains and the overall foot structure of living animals, hooves clearly are an important part of a living ungulate's foot structure, and their ability to locomote; thus being able to predict their size from skeletal remains is as much of a part of the goal of this study as predicting the areas of softer tissues (Warner, et al., 2013). In this sense, the term 'soft tissue' as used in this study refers to 'non-skeletal tissue', with the hardness of these tissues largely irrelevant.

Initially, we attempted to calculate the 2D convex hull (a shape made by joining the outermost data points in a simplified representation of the data (see figure 1C-D, in green)) of each silhouette, but found via pose tests using bird feet that this method was extremely sensitive to pose, particularly whether the digits were laterally spread or not (Supplementary material 1). Instead, 2D, tight-fitting alpha shapes (where the outermost data points were joined in a shape that most closely fits the silhouette's true shape (figure 1C-D, in pink)) were produced for each silhouette, and the area of these alpha shapes calculated. The alphaShape command in MatLab uses an 'alpha value' to determine the maximum distance between edge points to bridge (a sufficiently large 'alpha value' will produce a convex hull). We used the automatically determined alpha value for each alpha shape, which is calculated based on the density of vertices in the model, as this produces the tightest fitting single shape for any given set of points. We set the hole threshold to be extremely large (larger than the foot as a whole) to remove any holes from the interior of the alpha shape. The surface area of the skeleton's alpha shape as a percentage of the skin's shape was then used to compare each organism.

The dataset was then run through PGLS (phylogenetic generalised least squares) regression analyses to assess the significance of the relationship between the variables, and how much impact common ancestry between the animals studied affected the results (Blomberg et al., 2012; Felsenstein, 1985). This was accomplished using Mesquite (Maddison and Maddison, 2001) to draw three simple trees (manually compiled "consensus" phylogenies based on the most recent and broadly accepted phylogenies at the time of writing, within which the placement of Carnivora, Cetartiodactyla and Perissodactyla in relation to each other, was the only major point of contention (Gauthier et al., 1988; Nery et al., 2012; Prum et al., 2015)) connecting the organisms involved in this study. We then applied the Grafen method (Grafen, 1989) of branch length estimation to the trees, and ran PGLS via the Ape (Paradis et al., 2004), Geiger (Harmon et al., 2008), Nlme (Bliese, 2006) and Phytools (Revell, 2012) packages in R software. Results for forefeet, hindfeet, and all feet were each tested. Skin and skeletal foot surface area were tested for correlation with body mass as part of the PGLS tests. P values <0.05 were considered significant. Body masses were taken from scan metadata where possible, or estimated from the literature (e.g. Dunning Jr, 1992) where such metadata were not available (Supplementary material 1).

Skin surface area was plotted against skeletal surface area for all analyses, using the entire data set, and then broken up into smaller groups: unguligrade, digitigrade, plantigrade, terrestrial, semi-aquatic, erect posture, sprawling posture, mammals, and birds. The plots were framed in terms of predictability of skeletal area from skin area, to emphasise potential utility for trackmaker identification from fossils. However, this data is intended to be interpretable both ways, and the prediction of *in vivo* surface area from skeletal remains is of equal utility. For the purposes of these analyses, the digitigrade (Pose 2a) and plantigrade (Pose 2c) poses of semi-digitigrade/subunguligrade (*sensu* Carrano, 1997) animals were added to their respective groups, whereas Pose 2b was used for the remaining

groups, as it represents an intermediate pose. Semi-aquatic included amphibians, crocodilians and hippopotamuses, terrestrial did not include birds except for *Dromaius novaehollandiae*, and sprawling (here meaning non-erect) posture included amphibians, lepidosaurs and crocodilians, although crocodilians use a range of limb postures spanning the sprawling-to-erect continuum (Gatesy, 1991; Reilly and Elias, 1998).

Results

For the Pose 1 analysis (approximate life position), projected foot skeleton surface area as a percentage of projected fully fleshed foot surface area (Figure 2, above cladogram) was an average of 56% (both mean and median) for all organisms measured (three amphibians, four crocodilians, seven birds, and fourteen mammals), with means of 49% for amphibians (53% median), 47% for crocodilians (48% median), 68% for birds (67% median), and 55% for mammals (54% median) with an average standard deviation of 13%. Extremely similar results were found with bones oriented as in Pose 2. The smallest percentages of skeletal vs. fleshed surface area observed were in *Equus* species (*Equus quagga* at 34%, *Equus ferus caballus* 38%), *Giraffa camelopardalis* (38%), *Crocodylus niloticus* (38%), and *Cryptobranchus alleganiensis* (39%). However, besides *Equus* and *Giraffa*, other ungulates did not stand out as having particularly low skeletal areas relative to skin areas. Carnivorans had proportionately high skeletal calculated area. The highest skeletal areas relative to skin areas (as seen from the underside, and in two dimensions) were *Coturnix coturnix* at 83%, followed by *Panthera leo persica* and *Ceratotherium simum*, at 81% and 73%, respectively.

Where skeletal models were set flat (Pose 2), all unguligrade animals expressed lower skeletal area compared to skin surface area, compared with Pose 1 (Figure 2). The zebra stood out most with just 22% skeletal representation.

Elephas, Hippopotamus, and *Ceratotherium* showed considerable variability depending on which foot bones (Pose a/b/c) were used to predict skeletal area: *Hippopotamus* (37/76/100%), *Ceratotherium* (31/74/98%), *Elephas* (17/42/68%). 100% skeletal surface area representation in the hippopotamus clearly suggests that treating these animals as plantigrade does not yield results representative of these animals' foot morphology, or indeed results that are useful for predictive purposes, especially given the steep (subvertical) angle at which these animals position their feet *in situ*.

Carnivorans, particularly cats, typically do not have their digits extended fully when walking or standing, as such relative skeletal area calculated from Pose 2 (eg. *Panthera* 93%, *Vulpes* 92%) generally produces higher relative skeletal areas than the more life-like Pose 1 (eg. *Panthera* 81%, *Vulpes* 70%) .

Overall, mammalian data were highly variable (47% range from maximal to minimal values in Pose 1, over 80% range in Pose 2). Given that mammals had the most species represented in this study (then birds, then crocodilians), is it unclear whether variability within other groups would increase to the same level, with more data. REWORD?

Bird and crocodilian data were more consistent than mammals (25% range for birds in all analyses, 18% range for crocodilians). *Dromaius*, which was morphologically and

functionally distinct from the other birds in the study in terms of being large and flightless, fell neatly within the range for birds.

Raw numbers for projected skeleton and projected skin surface area, calculated from Pose 1, were plotted as a log graph, and a power trendline fitted (Figure 3). This plot, despite the variation seen in Figure 2, showed a strongly positive correlation ($R^2 = 0.99$, p value <0.05) in 'Pose 1' between skin and skeletal foot surface area. This correlation can be described with the formula $y = 0.59x^{0.9865}$ (where y = skeletal foot surface area and x = foot skin surface area). This skin and skeletal foot surface area's scaling relationship was close to isometry (slope of 1.0). Soft tissue surface area may therefore be predicted, on average, as approximately 1.67 times skeletal surface area. The majority of the data fitted the trendline tightly when log-transformed, and *Elephas* and *Ceratotherium* were the only animals that diverged notably from the linear trendline. If the three largest animals are removed from the data set, or the three smallest, the strength of the correlation is unaffected, but soft tissue area predictions from skeletal area decrease (Supplementary Material 1). If both groups are removed, the predicted value further lowers.

When the forelimb and hindlimb results were calculated separately, the formulae differed noticeably ($y = 0.52x^{0.9944}$ and $y = 0.64x^{0.9815}$ respectively). The difference in slope was not statistically significant, and R^2 values remain ~0.99 (Figure 3). However, soft tissue area was ~2 times skeletal area in the forelimb, but only ~1.56 times in the hindlimb. See Table 1 for full list of formulae and R^2 values.

For all flat pose analyses (Pose 2), heavier animals remained the outliers, with *Elephas, Hippopotamus,* and *Ceratotherium* diverging most from the trendline, whereas the rest of the data fit the trendline tightly (Figure 4). Similar to the Pose 1 analysis, Pose 2b suggested high predictability, with soft tissue as approximately 1.67 times skeletal surface area. Regressions for Pose 1 and Pose 2b were statistically similar. The analysis treating semi-digitigrade/sub-unguligrade as plantigrade (Pose 2c) suggested soft tissue as approximately 2.04 times skeletal surface area, and semi-digitigrade as digitigrade (Pose 2a) resulted in soft tissue as 1.05 times skeletal surface area. Interestingly, the hindlimbs-only regression for Pose 2b was significantly different from its equivalent with both fore- and hindlimbs and forelimbs-only (Table 1).

PGLS results (e.g. for all feet, in 'Pose 1', with Carnivora and Perissodactyla in a single clade) produced a correlation of -0.171, and a Pagel's lambda value ~1, with an adjusted R^2 of 0.92 (t-statistic 18.06, residual S.E. 12005, 29 DF (26 residual)). Similar results were found when running the same tests on fore-and hind-feet separately, with the other two phylogenetic tree arrangements. With all these arrangements where skeletal elements were laid flat, variable adjusted R^2, Pagel's lambda (though all ~1), and t-statistics were found, with higher standard error (15686.49 SE (28 DF (26 residual)) in Pose 2a) (Supplementary material 1). Despite the variations, this still suggests that phylogeny is not the main driver of the correlations found.

Separate regressions for unguligrade, digitigrade, plantigrade, terrestrial, semi-aquatic, erect posture, sprawling posture, birds and mammals, all showed strong correlations (Table 2, Supplementary material 1 and 2). Equations for all the analyses varied, with opposing regressions (e.g. sprawling versus erect posture, or terrestrial versus semi-aquatic) statistically different from each other (Table 2). Although R^2 values suggest high correlations for these regressions, the lack of data points in each of them (particularly those with the highest R^2 values) suggests their predictive value is relatively low at present. There

314 are potentially functional reasons why, for example, sprawling animals, semi-aquatic
315 animals, and birds would have stronger correlations and more predictable foot
316 morphologies, but the lower scores in groups with more data points suggests high
317 correlation in groups with few data points may be an artefact, and should be viewed with
318 caution.

319 Body mass had no significant effect on relative skin/skeletal areas. This was unsurprising
320 because *Ceratotherium* results indicated more skeletal representation than other large
321 animals such as *Elephas*, and percentage of skeletal vs. non-skeletal (skin) area results for
322 small animals did not appear to skew towards either obviously high or low skeletal
323 representation (Supplementary Material 1).

324

325 **Discussion**

326 Projected skeletal surface area as a percentage of projected skin surface area varied
327 between the organisms studied, most notably in mammals, which yielded both the lowest
328 and second highest values (Figure 2). Bird feet are all similarly digitigrade in their posture
329 and are largely made up of skeleton (with three major digits and consistent phalangeal
330 numbers), skin, and connective tissue, so their more consistent percentages are not
331 surprising considering that some of the mammals in this dataset had hooves, fatty footpads,
332 and a wide range of foot anatomies and postures (from plantigrade to unguligrade). PGLS
333 results suggested that the correlation between skin and skeletal foot surface area in all
334 poses, as well as being very strong, were not significantly affected by phylogeny. This
335 suggestion was supported by Figures 3 and 4, in which the majority of data points fitted
336 neatly around the trendline.

337 *Equus* and *Giraffa* stood out in this dataset for having an especially low relative skeletal
338 surface area. All extant horses have one toe with a large, keratinous hoof (Bowker et al.,
339 1998), so this was perhaps to be expected. Giraffes also have relatively small feet and
340 gracile legs compared to other animals of similar size, and a combination of high body
341 mass and high running speeds, which contribute to an overall unique morphology (van
342 Sittert et al., 2015). Pose 2 resulted in a lower relative skeletal area across unguligrade
343 animals, though none as extreme as either *Equus* species. By focusing on ungual bones, it
344 became clear that the keratinous sheath that forms the hoof dominates the 'silhouettes',
345 with skeletal tissue only represented by the very tip of the toe, so this is to be expected.
346 Non-unguligrade ungulates: *Ceratotherium, Hippopotamus*, *Camelus dromedaries, and*
347 *Vicugna pacos*, did not yield similar results to unguligrade ungulates, and varied
348 significantly from this group, as well as from each other.

349 For *Crocodylus niloticus*, the fact that crocodiles have relatively thin, long, digital bones,
350 somewhat similar to human phalanges, that converge to form a surprisingly robust foot,
351 could have some effect (Ferraro and Binetti, 2014). Furthermore, joint range of motion
352 studies have suggested an unusual wrist function and resultant manus posture in
353 crocodilians favouring rigidity, which could affect potential foot contact area (Hutson and
354 Hutson, 2014). This rigidity could potentially aid in swimming, with the stiff foot acting in
355 a flipper-like fashion to push through water efficiently, which smaller crocodilians tend to
356 rely upon (Seebacher, et al., 2003). Furthermore, the *Crocodylus niloticus* specimen used
357 was the only juvenile in this study, and its phalanges were small and spaced far apart in
358 some cases, so this result could be an artefact of ontogeny, or the quality of the models

used. Further studies on the effect of ontogeny on skeleton to skin surface area ratio could elucidate this further. Indeed, in future studies consideration should be given to levels of ossification of manus and pes bones. For example, our *Cryptobranchus* CT scan was missing wrist bones on all feet when segmented because these elements were cartilaginous in the specimen scanned, and were indistinguishable from soft tissue. Such ossification is likely to vary across species, and across ontogeny.

At the other extreme, where skeletal surface area was high (most closely approaching projected skin surface area), several birds (most notably *Coturnix*, *Accipiter nisus*, and *Alectoris chukar*) along with carnivorans and *Ceratotherium* (as well as *Hippopotamus* in Pose 2b and 2c) stand out the most. For birds, this is understandable considering their relative lack of musculature and fat in their feet. For carnivorans this could be explained by their claws, extending beyond the main body of the foot, by the resting position of their digits *in vivo,* and by their footpads, for which stiffness scales directly with body mass, while foot contact area lags behind (Chi and Roth, 2010). This scaling allows carnivorans to maintain relatively small feet that are light enough to be moved quickly (Kilbourne and Carrier, 2016; Kilbourne and Hoffman, 2013).

Body mass seemed to have little general effect on the relationship between skin and skeletal foot surface area. Previous studies have found a scaling relationship between body mass and foot contact area not significantly different from isometry (Michilsens et al., 2009), implying that the ratio of skeleton to soft tissue in the foot was not affected by this scaling effect. The scaling relationship between the ratio of skin to skeletal foot surface area was at best trivially different from isometry– a sensible result given that the variables are two facets of the same structure (i.e. the manus or pes), and therefore their structure and development are intrinsically linked. Despite this result, the largest animals in our dataset were the most outlying (much less so when plotted logarithmically (Figure 3)). It is notable that these largest animals, namely, *Elephas, Ceratotherium,* and *Hippopotamus*, were also the only semi-digitigrade/subunguligrade animals in our data. These animals both had the largest feet in the study and possess fatty foot pads to reduce loads on their individual toes and spread out underfoot pressure due to their large body masses (Hutchinson et al., 2011; Regnault et al., 2013). The divergence of the data for these animals appears to be influenced by their foot posture as well as their large size, with the adaptation of a semi-digitigrade posture potentially occurring specifically to support their large body weights.

It may be worth considering that beyond a certain weight threshold, specialised foot morphologies are necessary for weight support and locomotion, and thus successively heavier animals may have more disparate soft tissue structure and foot posture adaptations to cope with increased load (Hutchinson, et al., 2011). This has implications for the inherent predictability of our methods for very large extinct animals, such as sauropod dinosaurs, especially where foot posture is loosely inferred and little information about soft tissue structure is available. Follow-up studies on semi-digitigrade foot postures and how they support loads differently to other foot postures, as well as similar studies to this, using additional heavy and semi-digitigrade animals, would increase understanding of this variation of foot form and function. Contrary to the semi-digitigrade animals in our study, the giraffe, an unguligrade animal, was the largest other tetrapod (<1500kg vs. 3000+kg in larger individuals of the semi-unguligrade taxa), and deviated little from trendlines.

The strength of the correlation between skin and skeletal foot surface area, despite variations seen in Figure 2, implied sufficient reliability to predict one from the other (Figure 3). Most of the data fitted tightly around the trendline (Figure 3, Table 1).

406 However, birds only appeared above this line. Perhaps a more accurate correlation could be
407 achieved for birds alone with a larger avian dataset (with a wider range of foot sizes),
408 which would allow more accurate predictions of bird foot surface area, and of foot surface
409 area for animals with similar pedal anatomy to birds (such as non-avian theropod
410 dinosaurs). Although our main results could be refined with a much larger tetrapod data set,
411 it appears that foot skin surface area can be predicted from foot skeletal surface area, with
412 soft tissue generally predictable as approximately 1.67 times skeletal foot surface area, as
413 demonstrated in Poses 1 and 2b. However, when analyzed separately, manus and pes
414 presented differing ratios, with soft tissue surface area of the former being predicted as ~2
415 times skeletal area, but just ~1.56 times for the pes. This correlation could potentially be
416 used to estimate skeletal foot surface area of animals from their footprints, and its inverse
417 used to predict skin-on-foot surface area of extinct animals from their skeletons, and even
418 of cadavers from skeletons, with potential forensic applications.

419 For Pose 2, *Elephas, Ceratotherium,* and *Hippopotamus* were tested in three different
420 poses. Their foot anatomy is unusual in that they have a foot posture with most foot
421 elements far off the ground, but also have fatty pads which give them a large foot surface
422 area. With this in mind, all foot elements being in line with the horizontal plane, as in Pose
423 2c, is highly unrealistic. Pose 2a is perhaps more realistic than 2c, but assumes fewer foot
424 elements are supportive during stance than is accurate *in vivo*. The most representative
425 position for semi-digitigrade would arguably be Pose 1, as this did not force these animals
426 into an unrealistic foot posture. However, both Pose 1, and Pose 2b both result in the same
427 1.67 times skeletal surface area value, and Pose 2b's intermediate nature tests a pose in
428 between digitigrade and plantigrade. Pose 2b then, is perhaps the best repeatable method.
429 If, despite this, our other methods were chosen to predict foot surface area, skin surface
430 area would be equal to 1.05 times skeletal surface area for Pose 2a, and 2.04 times skeletal
431 surface area for Pose 2c. The variability in these analyses does reveal that altering the
432 results of the largest animals in the study alters the equation used. Therefore, perhaps this
433 method would be best applied to smaller and non-semi-digitigrade animals. However,
434 variation in area results is to be expected when fundamentally changing the number of
435 skeletal elements in an analysis.

436 Where data were divided into smaller groups for analysis, strong correlations were found in
437 results for plantigrade animals, semi-aquatic animals, sprawling posture, and birds (Table
438 2). Selective pressures potentially could drive a need for similar foot anatomy across these
439 groups, and therefore predictable foot structures, such as adaptations for perching,
440 swimming, and supporting body weight when feet are not directly under the body. Yet
441 considering that these groups were also the groups with the fewest data points, we cannot
442 draw any definitive conclusions from these results.

443 In terms of methods used, we found that convex hulls are highly sensitive to foot pose,
444 such as the size of inter-digital angles (Supplementary material 1), a result consistent with
445 previous findings (Cholewo and Love, 1999). This could be the cause of wide error
446 margins if these hulls were used for predictive purposes. This is especially relevant in re-
447 posed foot models, where inter-digital angles are manipulated to resemble *in vivo*
448 arrangements, and in animals that have long, thin digits, such as crocodilians. Alpha shapes
449 produced more consistent, 'tight-fitting' outlines for area calculation, a much more accurate
450 measure of the real scope of foot surface area for these models.

451 Inevitably, models derived from CT scans, such as those we used, ignore certain *in vivo*
452 factors such as foot deformation during contact with the ground. While we attempted to

stick closely to the *in situ* positions of feet (Pose 1), and aimed for a more objective iteration of our analysis by laying bones flat to remove subjectivity (Pose 2), deformation is a very difficult issue to control for. Collection of the data needed to account for this would require advanced *in vivo* imaging techniques such as biplanar fluoroscopy (i.e. "XROMM"; Brainerd et al., 2010; Gatesy et al., 2010); however, such techniques remain limited in the size of potential subjects (e.g. Panagiotopoulou et al., 2016) and can be expensive and time-consuming to conduct. Despite this issue, deformation of the foot should generally not be significant enough that it should diminish the usefulness of this study or the predictability of the methods employed here, as even in soft footpads, foot contact area does not maintain constant stress with body mass, and larger body mass can lead to increased foot stiffness (Chi and Roth, 2010). Combining this methodology with XROMM data for elephants and other animals with large, fatty foot pads, however, would be a boon to determining the overall effect of deformation on the predictability of these methods and on foot surface area in general, as this particular aspect of foot anatomy is the most prone to deformation with body weight, due to its high compliance (Hutchinson, et al., 2011). Overall, CT scans are a reliable resource for studies like these, and their utility in determining foot surface area could potentially contribute to future studies on animal locomotion and posture if used in conjunction with *in vivo* loading, centre of mass and pressure data. However, as in this study, where quality of the models varied, results could potentially be limited by the fidelity of the scans available, and therefore, more scans available for each animal to have the option to pick and choose the most complete and highest quality, as well as more computing power and high-end software, would be a boon to future studies.

Most studies concerning underfoot areas and pressures have focused on humans and other primates. Adaptations for arboreal locomotion have resulted in large functional differences between the forelimb and hindlimb in primates (Schmitt and Hanna, 2004). Such differences, would make them an interesting subject for a follow-up study.

Assigning specific trackmakers to fossilised trackways is a difficult task (Falkingham, 2014). It is our hope that these results could be used to constrain potential trackmaker identity. However, as an extrapolation from a bivariate plot, with a number of variables unaccounted for such as soft tissue and substrate compliance, the applications of figure 3 and its predictions are currently limited, and such identifications of trackmakers must be undertaken cautiously.

When predicting the skeletal surface area of the feet of extinct animals, and identifying trackmakers, the many complexities of footprint formation must be taken into account. The shape of footprints is influenced by foot pressures (Hatala et al., 2013), centre of mass (Castanera et al., 2013), style of locomotion (Hatala et al., 2016), and crucially, substrate type (Morse et al., 2013; Gatesy and Falkingham, 2017). In addition, fossil footprints can be distorted by geophysical pressure (Lockley and Xing, 2015) and by fluid intrusion and other natural processes of the rock cycle (Knaust and Hauschke, 2004). Even when footprints are first made, the impression left is rarely of the whole foot (Li et al., 2008; Gatesy and Falkingham, 2017) and the parts of the foot exerting the most pressure are most likely to be preserved in a substrate (Jackson et al., 2009). With that said, the size and shape of feet is consistently considered one of the three most important defining influences of footprint formation (Falkingham, 2014; Minter et al., 2007; Padian and Olsen, 1984). That foot size and shape is the focus of this study, the findings herein concern matters of critical importance to footprint formation and trackmaker identification.

When trying to model footprint formation and dynamics of extinct animals, centre of mass and underfoot pressures of the animals in question are determining factors. When considering these factors, the difference between manus and pes size and pressure is of great importance. Disparity between the anterior and posterior parts of the body is especially notable as previous biomechanical models have often underestimated mass in the cranial half of the body (Allen et al., 2009). Simply put, taking into account the differences between soft tissue area in manus and pes could make a notable difference in estimations of underfoot pressures and simulations of footprint formation. As an example, when the skeletal remains of *Plateosaurus engelhardti* feet were laid flat, and their skin areas predicted from alpha hulls, estimated manus skin area was 32% of pes area when using the 1.67 multiplier from combined analyses, and 40% of pes area using the separate multipliers (2 for manus, 1.6 for pes). Using body mass and centre of mass calculations from(Allen et al., 2013), this results in predicted manus underfoot pressure of 80% pes pressure when combined, and 64% when separate (Supplementary Material 1). This effect should also be considered in the inverse when considering trackmaker anatomy from fossil footprints. In this way, this method is a useful tool to consider in digital reconstruction and trackmaker identification.

Conclusions

The surface areas of the skin of the foot *in situ* and of the foot's skeletal components are strongly correlated and thus should be predictable in terrestrial tetrapods. Skin surface area was approximately 1.67 times that of skeletal surface area (~2 times for manus, ~1.6 times for pes, if analysed separately). This trend was not affected by body mass and showed little evidence of being strongly affected by phylogeny. This predictability has potential in aiding with estimating the size and possible species of trackmakers in the fossil record, both by estimating the size of skeletal feet using footprints, and by estimating foot size, and therefore potential footprint size, from fossil feet.

Acknowledgements

We thank David Blackburn at the Florida Museum of Natural History for provision of frog CT scans, and Ryan Marek and Ikuko Tanaka, and several members of the Structure and Motion Lab for constructive comments. Thanks to Diego Pol and two anonymous reviewers for constructive critique and feedback. Thanks to Phylopic.org silhouette providers Steven Traver, T. Michael Keesey, Mattia Manchetti, Yan Wong, B. Kimmel, Jan A. Venter, Herbert H. T. Prins, David A. Balfour, Rob Slotow, Shyamal, and Elisabeth Östman – images used under their respective creative commons licenses.

Author Contributions

Research and analysis was conducted by ECS. Manuscript and figures by ECS, with contributes from PLF, JRH, and DMW. The majority of the CT scans used were provided by JRH. Research was part of a PhD by ECS, supervised by PLF DMW and JRH.

References

542 Alexander, R. M., 2004. Bipedal animals, and their differences from humans. J. Anat. 204,
543 321-330.
544 Alexander, R. M., Bennet, M. B., Ker, R. F., 1986. Mechanical properties and function of
545 the paw pads of some mammals. J. Zool. Lond. 209, 405-419.
546 Allee, W.C., Schmidt, K., 1937. Ecological animal geography. John Wiley and Sons.
547 Allen, J.A., 1877. The influence of physical conditions in the genesis of species. Radic.
548 Rev. 1, 108–140.
549 Astley, H. C., Roberts, T. J., 2014. The mechanics of elastic loading and recoil in anuran
550 jumping. J. Exp. Biol. 217, 4372-4328.
551 Bates, K.T., Mannion, P.D., Falkingham, P.L., Brusatte, S.L., Hutchinson, J.R., Otero, A.,
552 Sellers, W.I., Sullivan, C., Stevens, K.A., Allen, V., 2016. Temporal and
553 phylogenetic evolution of the sauropod dinosaur body plan. R. Soc. Open Sci. 3,
554 150636.
555 Bejan, A., Marden, J.H., 2006. Unifying constructal theory for scale effects in running,
556 swimming and flying. J. Exp. Biol. 209, 238–248.
557 Biewener, A.A., 1989. Mammalian terrestrial locomotion and size. Bioscience 39, 776–
558 783.
559 Birn-Jeffery, A.V., Hubicki, C.M., Blum, Y., Renjewski, D., Hurst, J.W., Daley, M.A.,
560 2014. Don't break a leg: running birds from quail to ostrich prioritise leg safety and
561 economy on uneven terrain. J. Exp. Biol. 217, 3786–3796.
562 Blackburn, T.M., Gaston, K.J., Loder, N., 1999. Geographic gradients in body size: a
563 clarification of Bergmann's rule. Divers. Distrib. 5, 165–174.
564 Bliese, P., 2006. Multilevel Modeling in R (2.2)–A Brief Introduction to R, the multilevel
565 package and the nlme package. October.
566 Blomberg, S.P., Lefevre, J.G., Wells, J.A., Waterhouse, M., 2012. Independent contrasts
567 and PGLS regression estimators are equivalent. Syst. Biol. 61, 382–391.
568 Bonnan, M. F., Shulman, J., Varadharajan, R., Gilbert, C., Wilkes, M., Horner, A.,
569 Brainerd, E., 2016. Forelimb kinematics of rats using XROMM, with implications
570 for small eutherians and their fossil relatives. PloS one 11.
571 Bowker, R.M., Van Wulfen, K.K., Springer, S.E., Linder, K.E., 1998. Functional anatomy
572 of the cartilage of the distal phalanx and digital cushion in the equine foot and a
573 hemodynamic flow hypothesis of energy dissipation. Am. J. Vet. Res. 59, 961–968.
574 Brainerd, E.L., Baier, D.B., Gatesy, S.M., Hedrick, T.L., Metzger, K.A., Gilbert, S.L.,
575 Crisco, J.J., 2010. X-ray reconstruction of moving morphology (XROMM):
576 precision, accuracy and applications in comparative biomechanics research. J. Exp.
577 Zool. Part Ecol. Integr. Physiol. 313, 262–279.
578 Carrano, M. T., 1997. Morphological indicators of foot posture in mammals: a
579 statistical and biomechanical analysis. Zool. J. Linnean Soc. 121, 77-104.
580 Castanera, D., Vila, B., Razzolini, N.L., Falkingham, P.L., Canudo, J.I., Manning, P.L.,
581 Galobart, À., 2013. Manus track preservation bias as a key factor for assessing
582 trackmaker identity and quadrupedalism in basal ornithopods. PLoS One 8, e54177.
583 Cheung, J.T.M., Zhang, M., Leung, A.K.-L., Fan, Y.-B., 2005. Three-dimensional finite
584 element analysis of the foot during standing—a material sensitivity study. J.
585 Biomech. 38, 1045–1054.
586 Chi, K.J., Roth, V.L., 2010. Scaling and mechanics of carnivoran footpads reveal the
587 principles of footpad design. J. R. Soc. Interface 7, 1145–1155.
588 Cholewo, T.J., Love, S., 1999. Gamut boundary determination using alpha-shapes, in:
589 Color and Imaging Conference. Society for Imaging Science and Technology, pp.
590 200–204.

591 Clack, J.A., 1997. Devonian tetrapod trackways and trackmakers; a review of the fossils
592 and footprints. Palaeogeogr. Palaeoclimatol. Palaeoecol. 130, 227–250.
593 Clarke, KA., 2017. Principles of thermal ecology. Oxford University Press.
594 Coombs Jr, W. P., 1978. Theoretical aspects of cursorial adaptations in dinosaurs.
595 Quarterly Rev. Biol. 53, 393-418.
596 Dunning Jr, J.B., 1992. CRC handbook of avian body masses. CRC press.
597 Falkingham, P.L., 2014. Interpreting ecology and behaviour from the vertebrate fossil track
598 record. J. Zool. 292, 222–228.
599 Falkingham, P.L., Bates, K.T., Mannion, P.D., 2012. Temporal and palaeoenvironmental
600 distribution of manus-and pes-dominated sauropod trackways. J. Geol. Soc. 169,
601 365–370.
602 Falkingham, P.L., Bates, K.T., Margetts, L., Manning, P.L., 2011a. The 'Goldilocks'
603 effect: preservation bias in vertebrate track assemblages. J. R. Soc. Interface 8,
604 1142–1154.
605 Falkingham, P.L., Bates, K.T., Margetts, L., Manning, P.L., 2011b. Simulating sauropod
606 manus-only trackway formation using finite-element analysis. Biol. Lett. 7, 142–
607 145.
608 Falkingham, P.L., Gatesy, S. M., 2014. The birth of a dinosaur footprint: Subsurface 3D
609 motion reconstruction and discrete element simulation reveal track ontogeny. PNAS
610 111, 18279-18284.
611 Farley, C.T., Glasheen, J., McMahon, T.A., 1993. Running springs: speed and animal size.
612 J. Exp. Biol. 185, 71–86.
613 Farlow, J.O., 1992. Sauropod tracks and trackmakers: integrating the ichnological and
614 skeletal records. Zubia 10.
615 Fedak, M.A., Heglund, N.C., Taylor, C.R., 1982. Energetics and mechanics of terrestrial
616 locomotion. II. Kinetic energy changes of the limbs and body as a function of speed
617 and body size in birds and mammals. J. Exp. Biol. 97, 23–40.
618 Felsenstein, J., 1985. Phylogenies and the comparative method. Am. Nat. 125, 1–15.
619 Ferraro, J.V., Binetti, K.M., 2014. American alligator proximal pedal phalanges resemble
620 human finger bones: Diagnostic criteria for forensic investigators. Forensic Sci. Int.
621 240, 151–e1.
622 Full, R.J., Kubow, T., Schmitt, J., Holmes, P., Koditschek, D., 2002. Quantifying dynamic
623 stability and maneuverability in legged locomotion. Integr. Comp. Biol. 42, 149–
624 157.
625 Garland, T., 1983. The relation between maximal running speed and body mass in
626 terrestrial mammals. J. Zool. 199, 157–170.
627 Gatesy, S. M., 1991. Hind limbs movements of the American alligator *(Alligator*
628 *mississippiensis)* and postural grades. J. Zool. 224, 577-588.
629 Gatesy, S.M., Baier, D.B., Jenkins, F.A., Dial, K.P., 2010. Scientific rotoscoping: a
630 morphology-based method of 3-D motion analysis and visualization. J. Exp. Zool.
631 Part Ecol. Integr. Physiol. 313, 244–261.
632 Gatesy, S.M., Biewener, A.A., 1991. Bipedal locomotion: effects of speed, size and limb
633 posture in birds and humans. J. Zool. 224, 127–147.
634 Gatesy, S.M., Falkingham, P.L., 2017. Neither bones nor feet: track morphological
635 variation and 'preservation quality.' J. Vertebr. Paleontol. e1314298.
636 Gatesy, S.M., Middleton, 2003. Skin impression microtopography in Triassic theropod
637 tracks. J. Vertebr. Paleontol. 23, 54A-54A.
638 Gatesy, S.M., Middleton, K. M., Jenkins Jr, F. A., Shubin, N. H., 1999. Three-dimensional
639 preservation of foot movements in Triassic theropod dinosaurs. Nature 399, 141–
640 144.

641 Gauthier, J., Kluge, A.G., Rowe, T., 1988. Amniote phylogeny and the importance of
642 fossils. Cladistics 4, 105–209.
643 Geyer, H., Seyfarth, A., Blickhan, R., 2006. Compliant leg behaviour explains basic
644 dynamics of walking and running. Proc. R. Soc. Lond. B Biol. Sci. 273, 2861–2867.
645 Grafen, A., 1989. The phylogenetic regression. Philos. Trans. R. Soc. Lond. B. Biol. Sci.
646 326, 119–157.
647 Harmon, L.J., Weir, J.T., Brock, C.D., Glor, R.E., Challenger, W., 2008. GEIGER:
648 investigating evolutionary radiations. Bioinformatics 24, 129–131.
649 Hatala, K.G., Dingwall, H.L., Wunderlich, R.E., Richmond, B.G., 2013. The relationship
650 between plantar pressure and footprint shape. J. Hum. Evol. 65, 21–28.
651 Hatala, K.G., Wunderlich, R.E., Dingwall, H.L., Richmond, B.G., 2016. Interpreting
652 locomotor biomechanics from the morphology of human footprints. J. Hum. Evol.
653 90, 38–48.
654 Heckel, F., Schwier, M., Peitgen, H.-O., 2009. Object-oriented application development
655 with MeVisLab and Python. GI Jahrestag. 154, 1338–51.
656 Henderson, D.M., 2006. Burly gaits: centers of mass, stability, and the trackways of
657 sauropod dinosaurs. J. Vertebr. Paleontol. 26, 907–921.
658 Hildebrand, M., 1980. The adaptive significance of tetrapod gait selection. Am. Zool. 20,
659 255–267.
660 Hinterhofer, C. H., Stanek, C. H., Haider, H., 2000. The effect of flat horseshoes, raised
661 heels and lowered heels on the biomechanics of the equine hoof assessed by finite
662 element analysis (FEA). J. Vet. Med. 47, 73-82.
663 Hodgins, J.K., Raibert, M.N., 1991. Adjusting step length for rough terrain locomotion.
664 IEEE Trans. Robot. Autom. 7, 289–298.
665 Hutchinson, J.R., Delmer, C., Miller, C.E., Hildebrandt, T., Pitsillides, A.A., Boyde, A.,
666 2011. From flat foot to fat foot: structure, ontogeny, function, and evolution of
667 elephant “sixth toes.” Science 334, 1699–1703.
668 Hutson, J.D., Hutson, K.N., 2014. A repeated-measures analysis of the effects of soft
669 tissues on wrist range of motion in the extant phylogenetic bracket of dinosaurs:
670 implications for the functional origins of an automatic wrist folding mechanism in
671 Crocodilia. The Anatomical Record 297, 1228-1249
672 Jackson, S.J., Whyte, M.A., Romano, M., 2009. Laboratory-controlled simulations of
673 dinosaur footprints in sand: a key to understanding vertebrate track formation and
674 preservation. Palaios 24, 222–238.
675 Kambic, R. E., Roberts, T. J., Gatesy, S. M., 2015. Guineafowl with a twist: asymmetric
676 limb control in steady bipedal locomotion. J. Exp. Biol. 218, 3836-3844.
677 Kilbourne, B.M., Carrier, D.R., 2016. Manipulated Changes in Limb Mass and Rotational
678 Inertia in Trotting Dogs (*Canis lupus familiaris*) and Their Effect on Limb
679 Kinematics. J. Exp. Zool. Part Ecol. Genet. Physiol. 325, 665–674.
680 Kilbourne, B.M., Hoffman, L.C., 2013. Scale effects between body size and limb design in
681 quadrupedal mammals. PLoS One 8, e78392.
682 Knaust, D., Hauschke, N., 2004. Trace fossils versus pseudofossils in Lower Triassic playa
683 deposits, Germany. Palaeogeogr. Palaeoclimatol. Palaeoecol. 215, 87–97.
684 Li, R., Lockley, M.G., Makovicky, P.J., Matsukawa, M., Norell, M.A., Harris, J.D., Liu,
685 M., 2008. Behavioral and faunal implications of Early Cretaceous deinonychosaur
686 trackways from China. Naturwissenschaften 95, 185–191.
687 Lockley, M.G., Farlow, J.O., Meyer, C.A., 1994. *Brontopodus* and *Parabrontopodus*
688 ichnogen. nov. and the significance of wide-and narrow-gauge sauropod trackways.
689 Gaia 10, 135–145.

690 Lockley, M.G., Xing, L., 2015. Flattened fossil footprints: implications for paleobiology.
691 Palaeogeogr. Palaeoclimatol. Palaeoecol. 426, 85–94.
692 Maddison, W.P., Maddison, D., 2001. Mesquite: a modular system for evolutionary
693 analysis.
694 McGuigan, M. R., Wilson, A. M., 2003. The effect of gait and digital flexor muscle
695 activation on limb compliance in the forelimb of the horse *Equus caballus.* J. Exp.
696 Biol. 206, 1325-1336.
697 McMahon, T.A., 1975. Using body size to understand the structural design of animals:
698 quadrupedal locomotion. J. Appl. Physiol. 39, 619–627.
699 Michilsens, F., Aerts, P., Van Damme, R., D'Août, K., 2009. Scaling of plantar pressures
700 in mammals. J. Zool. 279, 236–242.
701 Miller, C.E., Basu, C., Fritsch, G., Hildebrandt, T., Hutchinson, J.R., 2008. Ontogenetic
702 scaling of foot musculoskeletal anatomy in elephants. J. R. Soc. Interface 5, 465–
703 475.
704 Morse, S.A., Bennett, M.R., Liutkus-Pierce, C., Thackeray, F., McClymont, J., Savage, R.,
705 Crompton, R.H., 2013. Holocene footprints in Namibia: the influence of substrate
706 on footprint variability. Am. J. Phys. Anthropol. 151, 265–279.
707 Nery, M.F., González, D.J., Hoffmann, F.G., Opazo, J.C., 2012. Resolution of the
708 laurasiatherian phylogeny: evidence from genomic data. Mol. Phylogenet. Evol. 64,
709 685–689.
710 Panagiotopoulou, O., Pataky, T.C., Day, M., Hensman, M.C., Hensman, S., Hutchinson,
711 J.R., Clemente, C.J., 2016. Foot pressure distributions during walking in African
712 elephants (*Loxodonta africana*). Open Sci. 3, 160203.
713 Panagiotopoulou, O., Pataky, T.C., Hill, Z., Hutchinson, J.R., 2012. Statistical parametric
714 mapping of the regional distribution and ontogenetic scaling of foot pressures
715 during walking in Asian elephants (*Elephas maximus*). J. Exp. Biol. 215, 1584–
716 1593.
717 Panagiotopoulou, O., Rankin, J. W., Gatesy, S. M., Hutchinson, J. R., 2016. A preliminary
718 case study of the effect of shoe-wearing on the biomechanics of a horse's foot.
719 PeerJ 4, e2164.
720 Paradis, E., Claude, J., Strimmer, K., 2004. APE: analyses of phylogenetics and evolution
721 in R language. Bioinformatics 20, 289–290.
722 Pataky, T.C., Caravaggi, P., Savage, R., Parker, D., Goulermas, J.Y., Sellers, W.I.,
723 Crompton, R.H., 2008. New insights into the plantar pressure correlates of walking
724 speed using pedobarographic statistical parametric mapping (pSPM). J. Biomech.
725 41, 1987–1994.
726 Patla, A.E., 2003. Strategies for dynamic stability during adaptive human locomotion.
727 IEEE Eng. Med. Biol. Mag. 22, 48–52.
728 Platt, B.F., Hasiotis, S.T., 2006. Newly discovered sauropod dinosaur tracks with skin and
729 foot-pad impressions from the Upper Jurassic Morrison Formation, Bighorn Basin,
730 Wyoming, USA. Palaios 21, 249–261.
731 Pollitt, C. C., 2004. Anatomy and physiology of the inner hoof wall. Clinical Techniques in
732 Equine Practice 3, 1, 3-21
733 Prum, R.O., Berv, J.S., Dornburg, A., Field, D.J., Townsend, J.P., Lemmon, E.M.,
734 Lemmon, A.R., 2015. A comprehensive phylogeny of birds (Aves) using targeted
735 next-generation DNA sequencing. Nature 526, 569–573.
736 Qian, Z., Ren, L., Ding, Y., Hutchinson, J.R., Ren, L., 2013. A dynamic finite element
737 analysis of human foot complex in the sagittal plane during level walking. PloS One
738 8, e79424.

739 Reilly, S. M., Elias, J. A., 1998. Locomotion in *Alligator mississippiensis*: kinematic
740 effects of speed and posture and their relevance to the sprawling-to-erect
741 paradigm. J. Exp. Biol 201, 2559-2574.
742 Regnault, S., Hermes, R., Hildebrandt, T., Hutchinson, J., Weller, R., 2013.
743 Osteopathology in the feet of rhinoceroses: lesion type and distribution. J. Zoo
744 Wildl. Med. 44, 918–927.
745 Revell, L.J., 2012. phytools: an R package for phylogenetic comparative biology (and other
746 things). Methods Ecol. Evol. 3, 217–223.
747 Rosenbaum, D., Hautmann, S., Gold, M., Claes, L., 1994. Effects of walking speed on
748 plantar pressure patterns and hindfoot angular motion. Gait Posture 2, 191–197.
749 Saitta, E. T., Rogers, C. , Brooker, R. A., Abbott, G. D., Kumar, S. , O'Reilly, S. S.,
750 Donohoe, P. , Dutta, S. , Summons, R. E., Vinther, J., 2017. Low fossilization
751 potential of keratin protein revealed by experimental taphonomy. Palaeontology, 60:
752 547-556.
753 Schaller, N. U., D'Août, K., Villa, R., Herkner, B., Aerts, P., 2011. Toe function and
754 dynamic pressure distribution in ostrich locomotion. J. Exp. Biol. 214, 1123-1130.
755 Schmitt, D., Hanna, J.B., 2004. Substrate alters forelimb to hindlimb peak force ratios in
756 primates. J. Hum. Evol. 46, 237–252.
757 Seebacher, F., Elsworth, P. G., Franklin, C. F. Ontogenetic changes of swimming
758 kinematics in a semi-aquatic reptile (*Crocodylus porosus*). Aus. J. Zool 51, 15-24.
759 Segal, A., Rohr, E., Orendurff, M., Shofer, J., O'Brien, M., Sangeorzan, B., 2004. The
760 effect of walking speed on peak plantar pressure. Foot Ankle Int. 25, 926–933.
761 Snyder, R.C., 1962. Quadrupedal and bipedal locomotion of lizards. Copeia 1952, 64–70.
762 Taylor, C.R., Shkolnik, A., Dmi'el, R., Baharav, D., Borut, A., 1974. Running in cheetahs,
763 gazelles, and goats: energy cost and limb configuration. Am. J. Physiol. Content
764 227, 848–850.
765 Van Sittert, S., Skinner, J., Mitchell, G., 2015. Scaling of the appendicular skeleton of the
766 giraffe (*Giraffa camelopardalis*). J. Morphol. 276, 503–516.
767 Warner SE, Pickering P, Panagiotopoulou O, Pfau T, Ren L, Hutchinson JR., 2013. Size-
768 Related Changes in Foot Impact Mechanics in Hoofed Mammals. PLoS ONE 8(1):
769 e54784
770 Witmer, L.M., Thomason, J.J., 1995. The extant phylogenetic bracket and the importance
771 of reconstructing soft tissues in fossils. Funct. Morphol. Vertebr. Paleontol. 1, 19–
772 33.
773
774

775 **Tables**

776 **Table 1 – Regressions and Confidence Intervals for Main Analyses**

Analysis	Linear Regression	Linear R^2	Log Regression	Log R^2	95% CI	P value
Pose 1 - All limbs	y = 0.5134x + 146.71	R^2 = 0.9371	$y = 0.5901x^{0.9865}$	R^2 = 0.9877	1.92293 ± 0.06186	<2.2E-16
Pose 1 - Forelimbs	y = 0.4504x + 641.27	R^2 = 0.9237	$y = 0.5196x^{0.9944}$	R^2 = 0.9888	1.916 ± 7.887E-02	3.27E-15
Pose 1 - Hindlimbs	y = 0.5868x - 292.02	R^2 = 0.9748	$y = 0.6419x^{0.9815}$	R^2 = 0.9872	1.9229 ± 0.0632	<2E-16
Pose 2a -All limbs	y = 0.2049x + 1303.8	R^2 = 0.815	$y = 0.8688x^{0.9126}$	R^2 = 0.9669	3.9266 ± 0.3584	1.93E-11
Pose 2a -Forelimbs	y = 0.214x + 1345.4	R^2 = 0.8479	$y = 0.6915x^{0.9311}$	R^2 = 0.9717	3.9614 ± 0.3954	8.68E-09
Pose 2a -Hindlimbs	y = 0.1908x + 1177.4	R^2 = 0.7939	$y = 1.0637x^{0.8924}$	R^2 = 0.9638	4.1603 ±0.4157	2.08E-10

Pose 2b - All limbs	y = 0.4849x + 436.75	R^2 = 0.8866	$y = 0.5841x^{0.9771}$	R^2 = 0.9699	1.856 ± 0.1199	5.98E-15
Pose 2b - Forelimbs	y = 0.5234x + 410.47	R^2 = 0.8937	$y = 0.4652x^{0.9985}$	R^2 = 0.9708	1.7074 ± 0.1388	3.39E-10
Pose 2b - Hindlimbs	y = 0.4392x + 535.85	R^2 = 0.8913	$y = 0.7066x^{0.9574}$	R^2 = 0.9695	2.029 ± 0.139	4.83E-14
Pose 2c - All limbs	y = 0.7396x - 700.51	R^2 = 0.9339	$y = 0.4919x^{1.0048}$	R^2 = 0.9663	1.279 ± 6.225E-02	<2.2E-16
Pose 2c - Forelimbs	y = 0.7852x - 1120.2	R^2 = 0.9511	$y = 0.4047x^{1.0217}$	R^2 = 0.9675	1.211 ± 6.473E-02	3.03E-13
Pose 2c - Hindlimbs	y = 0.6907x - 228.13	R^2 = 0.9206	$y = 0.5693x^{0.9918}$	R^2 = 0.9654	1.333 ± 7.677E-02	8.04E-16

Table 2 – Regressions and Confidence Intervals for Analysis Subgroups

Analysis	Linear Regression	Linear R^2	Log Regression	Log R^2	95% CI	P value
Unguligrade	y = 0.3648x - 593.56	R^2 = 0.9529	$y = 0.2694x^{1.0095}$	R^2 = 0.9714	2.6121 ± 0.2903	0.000844
Digitigrade	y = 0.1923x + 1823.1	R^2 = 0.8338	$y = 2.0231x^{0.836}$	R^2 = 0.9695	4.336 ± 0.537	2.02E-06
Plantigrade	y = 0.7408x + 1128.3	R^2 = 0.9607	$y = 0.3463x^{1.0633}$	R^2 = 0.9929	1.29686 ± 0.08747	1.25E-07
Terrestrial	y = 0.4539x + 491.99	R^2 = 0.9077	$y = 0.6787x^{0.9559}$	R^2 = 0.9121	1.9998 ± 0.1769	4.25E-08
Semi-aquatic	y = 0.7671x + 408.03	R^2 = 0.9982	$y = 0.4235x^{1.0253}$	R^2 = 0.9944	1.30129 ± 0.02233	4.26E-09
Erect Posture	y = 0.4812x + 588.49	R^2 = 0.891	$y = 0.9412x^{0.9285}$	R^2 = 0.9478	1.8517 ± 0.1486	1.37E-10
Sprawling Posture	y = 0.5062x - 19.695	R^2 = 0.9929	$y = 0.5028x^{0.9885}$	R^2 = 0.9954	1.96139 ± 0.06779	1.13E-07
Birds	y = 0.5901x + 32.247	R^2 = 0.9995	$y = 0.8673x^{0.9561}$	R^2 = 0.9866	1.69386 ± 0.01636	1.59E-09
Mammals	y = 0.4759x + 903.78	R^2 = 0.8733	$y = 0.566x^{0.9793}$	R^2 = 0.9059	1.8353 ± 0.2018	9.87E-07

781 **Figures and Legends**

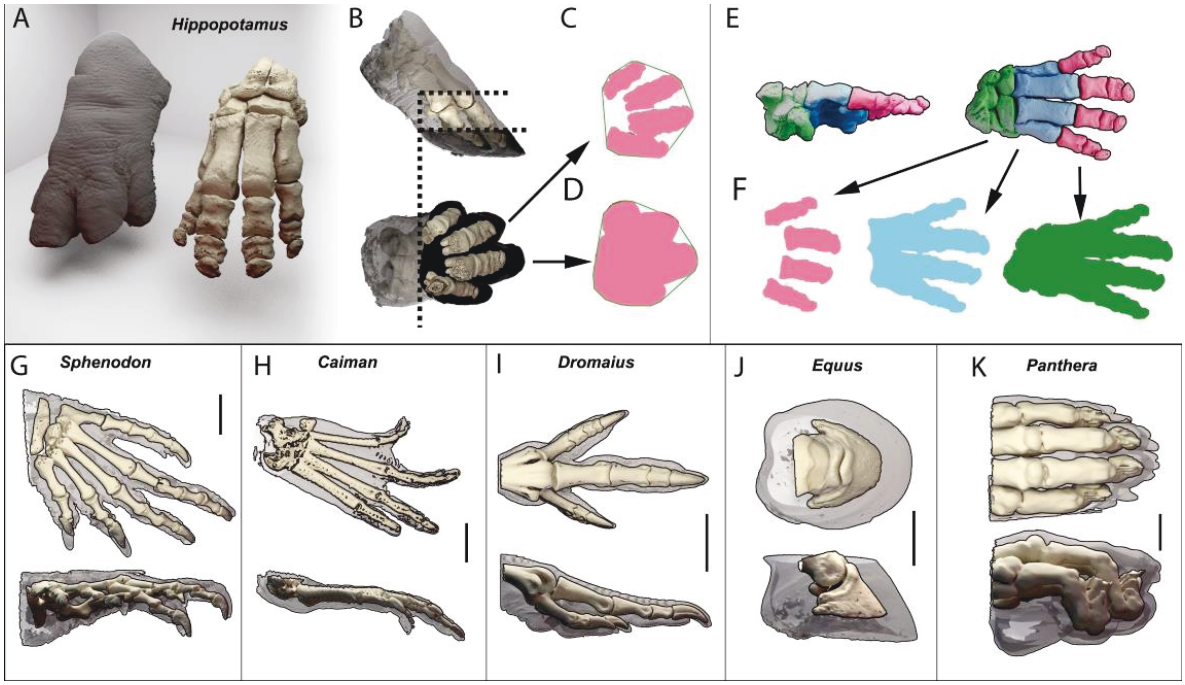

782
783 Figure 1 - Projected area calculated from 3D models. A) *Hippopotamus* Left forelimb, soft tissue and bones
784 reconstructed from CT data. B) The soft tissue was cropped at a point representative of the area that would
785 contact the ground during life. The bones were cropped based on the same posterior extent (pose 1). C) The
786 alpha shape (pink) and the convex hull (green) were used to determine underfoot area of the bones alone and
787 D) the soft tissue. E) Bones were laid flat for a more repeatable approach (pose 2). Where semi-digitigrade
788 animals were treated as digitigrade (pose 2a) only bones in pink were used, where semi-digitigrade animals
789 were treated as intermediate between digitigrade and plantigrade (pose 2b), blue and pink bones were used,
790 and where semi-digitigrade animals were treated as plantigrade, all bones including those in green were used.
791 F) Alpha shapes for poses 2a-c, where pink is 2a, blue is 2b, and green is 2c. G-K) Distinctive foot
792 morphologies in the data set. Scale bar = 10cm for all but G, where scale bar = 1cm.
793

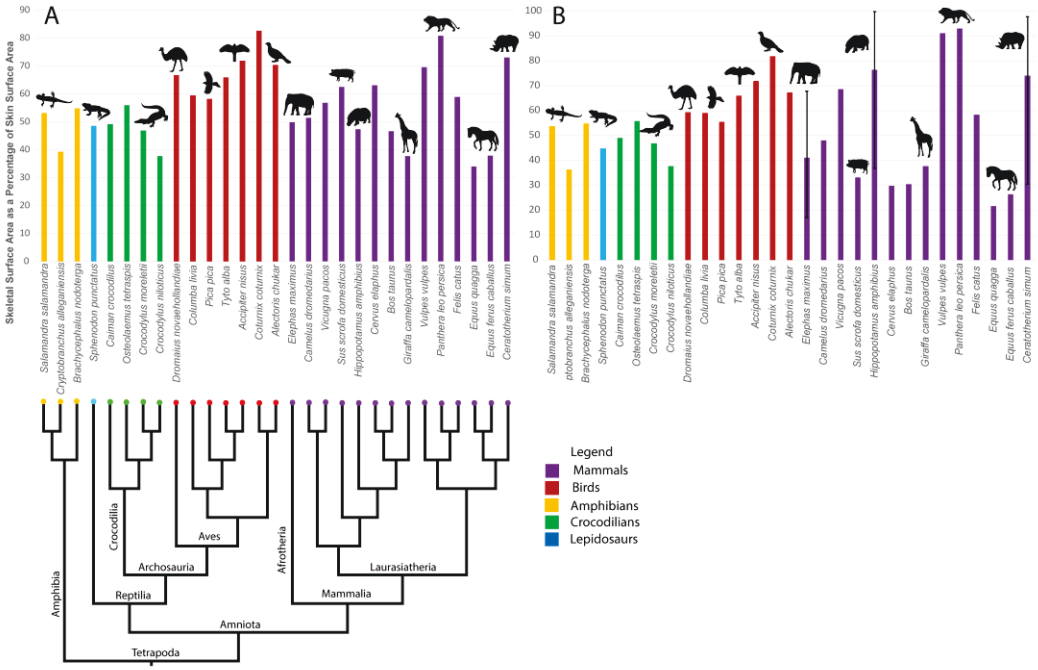

Figure 2 – Bar graph showing projected skin surface area as a percentage of projected skeletal surface area across all specimens in A) Pose 1, with phylogeny for context, and B) Pose 2 (for elephant, rhino, and hippo, main bar represents Pose 2b and additional bars show poses 2a and 2c). Silhouettes from Phylopic. Mammal data is in purple, bird data in red, crocodile data in green, lepidosaur data in blue, and amphibian in yellow.

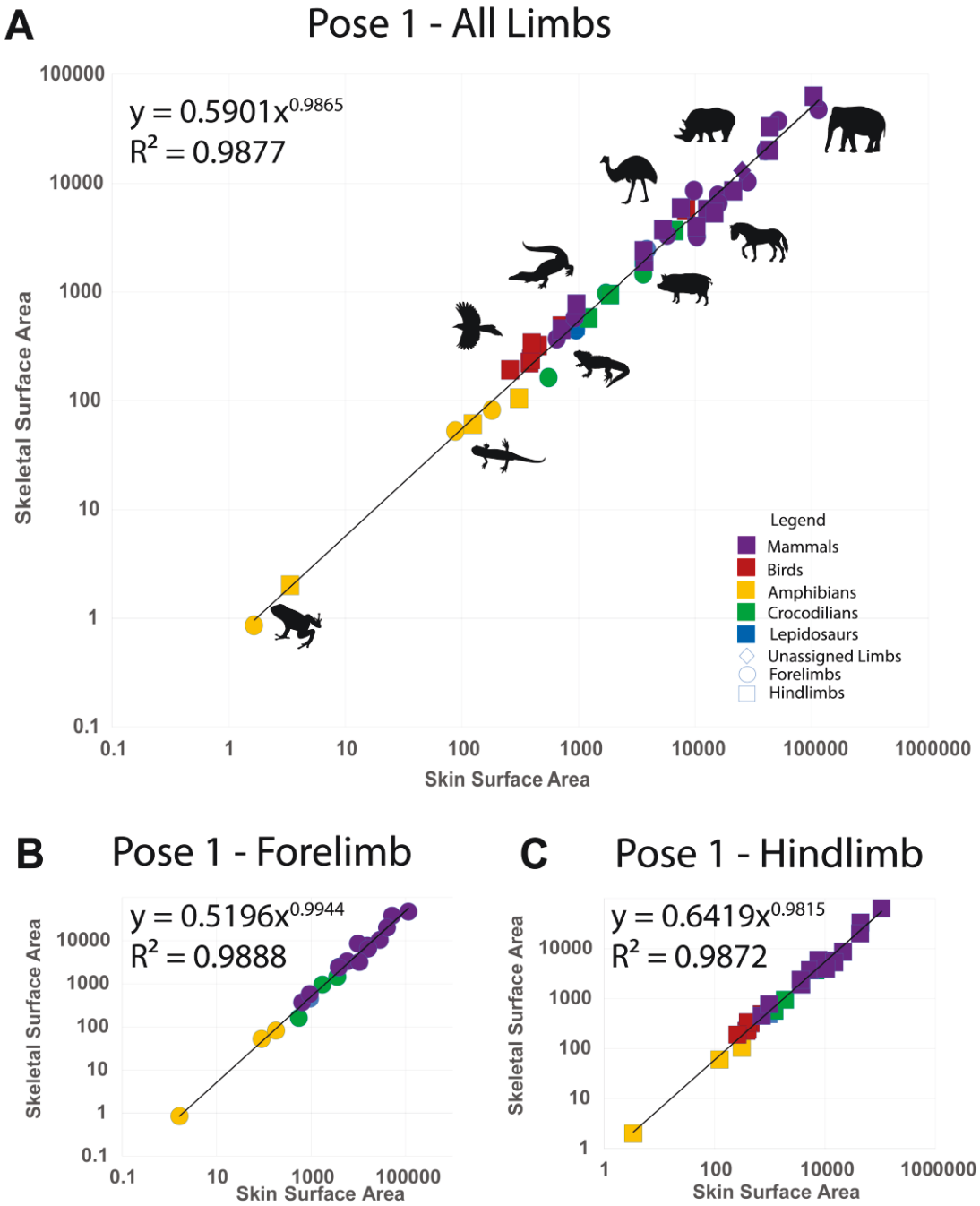

Figure 3 – Log_{10}-transformed plots for projected skin surface area against projected skeletal surface area in A) Pose 1, for all limbs, B) For Pose 1, for forelimbs, C) For Pose 1, for hindlimbs, Silhouettes from Phylopic. Mammal data is in purple, bird data in red, crocodile data in green, lepidosaur data in blue, and amphibian in yellow.

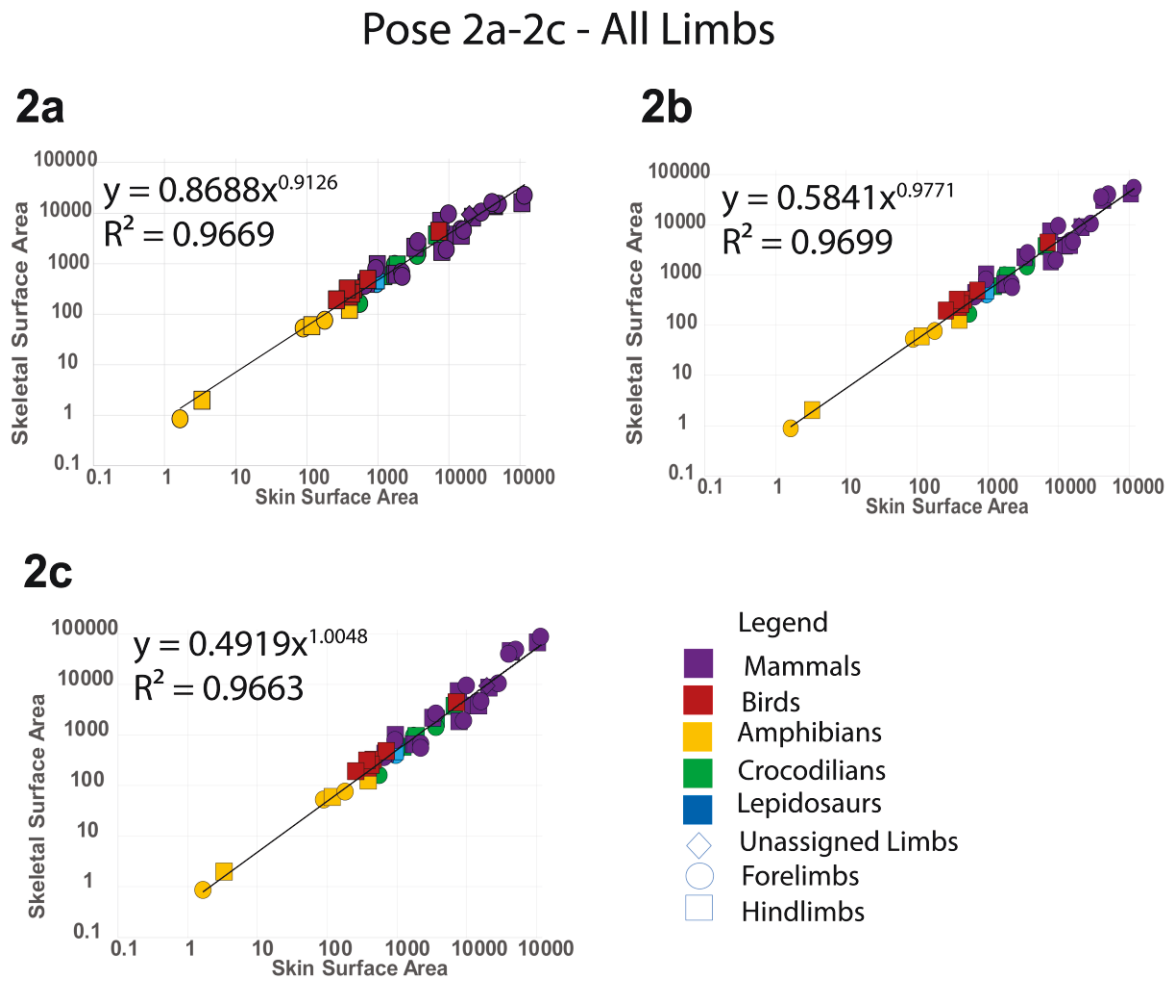

Figure 4 - Log_{10}-transformed plots for projected skin surface area against projected skeletal surface area for 2a) Pose 2a, all limbs, 2b) Pose 2b, all limbs, and 2c) For Pose 2c, all limbs. Silhouettes from Phylopic. Mammal data is in purple, bird data in red, crocodile data in green, lepidosaur data in blue, and amphibian in yellow.

Supplementary Figure Legends

Supplementary material 1: Supplementary tables – Additional data including p-values for all analysis, calculated soft-tissue and skeletal areas, approximate body masses for all animals.

Supplementary material 2: Supplementary graphs – Various plots for projected skin surface area against projected skeletal surface area in pose 1 and pose 2, presented as sub-groups by phylogeny and ecology.

Supplementary material 3: Supplementary outlines – Top-down projections of models used in study, showing alpha shapes and convex hulls.